Catalysis Today 149 (2010) 218–223

Contents lists available at ScienceDirect

Catalysis Today

journal homepage: www.elsevier.com/locate/cattod

Density functional theory study on adsorption of thiophene on TiO_2 anatase (0 0 1) surfaces

Jiahua Guo [a], Shingo Watanabe [a], Michael J. Janik [b], Xiaoliang Ma [a], Chunshan Song [a,b,*]

[a] Clean Fuels and Catalysis Program, the EMS Energy Institute, and Department of Energy and Mineral Engineering, The Pennsylvania State University, University Park, PA 16802, USA
[b] Department of Chemical Engineering, The Pennsylvania State University, University Park, PA 16802, USA

ARTICLE INFO

Article history:
Available online 12 June 2009

Keywords:
Adsorption
Desulfurization
DFT
Titanium oxide
TiO_2
Thiophene
Anatase

ABSTRACT

In order to develop a fundamental understanding of the adsorption mechanism of thiophenic compounds on TiO_2-based adsorbents for ultra-deep desulfurization of liquid hydrocarbon fuels, a density functional theory (DFT) study was conducted on the adsorption of thiophene over the TiO_2 anatase (0 0 1) surface. The perfect, O-poor (with oxygen vacancies), and O-rich (with activated O_2 on the surface) anatase (0 0 1) surfaces were built, and the interaction of thiophene molecule with these surfaces was examined. The adsorption configuration and adsorption energy on the different surfaces and sites were estimated. The results showed that thiophene may be adsorbed on both the perfect and O-poor surfaces through an interaction between the Ti cations on the surface and the S atom in thiophene, whereas on the O-rich surface through an interaction of the activated O atoms (the dissociatively or associatively adsorbed O_2) on the surface with the S atom in thiophene to form a sulfone-like surface species. The adsorption of thiophene on the O-rich surface is significantly stronger than adsorption on the perfect and O-poor surfaces on the basis of the calculated adsorption energies. The results indicate that the activated O_2 on the TiO_2 anatase (0 0 1) surface may play an important role in the adsorption desulfurization over the TiO_2-based adsorbents, and increased concentration of the activated O_2 on the surface may result in improvement of the adsorption capacity of the adsorbents.

1. Introduction

Ultra-deep desulfurization of liquid hydrocarbon fuels has become an increasingly important subject, as the quality of crude oils is getting poorer and the sulfur restriction of liquid fuels becoming tighter [1]. Currently, the regulations by the U.S. Environmental Protection Agency (EPA) limit the sulfur content to less than 30 and 15 parts per million by weight (ppmw) for gasoline and diesel, respectively. On the other hand, liquid hydrocarbon fuels are potential fuels for on-board or on-site H_2 production for automotive, residential and portable fuel cells due to their high energy density, wide availability and safety in storage. However, the sulfur compounds in the fuels poison the reforming and water-gas shift catalysts as well as the fuel cell electrodes. Thus, for fuel cell applications the sulfur concentration in liquid hydrocarbon fuels needs to be further reduced to 1.0 ppmw or less [2,3].

Hydrodesulfurization (HDS) is a conventional and dominant method in refineries worldwide for removing sulfur from liquid hydrocarbon steams. However, this process needs to be conducted at high temperature and high pressure in the presence of hydrogen. Especially for removing the refractory sulfur compounds (alkylated dibenzothiophene-type compounds), lower space velocity and higher H_2 pressure are required [3–5]. Also, in the deep HDS process, the olefins and aromatics in gasoline are hydrogenated partially, which results in a significant decrease of the octane number of gasoline and increase of hydrogen consumption. Therefore, several new approaches have been explored for ultra-deep desulfurization [5–7]. One of these alternative processes is the adsorptive desulfurization (ADS) [5,6], which has received a great attention for production of ultra-low sulfur fuel, due to its significant advantages including no hydrogen consumption, capability to remove the refractory sulfur compounds, and simple operating process [8]. Several types of materials have been studied as adsorbents, such as zeolites [9–12], reduced metals [13], metal oxides [14], and activated carbons [15].

A $Ti_{0.9}Ce_{0.1}O_2$ material was reported recently as a promising adsorbent for ADS of liquid hydrocarbon fuels [16]. This adsorbent offers good adsorption selectivity for sulfur compounds and good regenerability by using air. By XRD study, Watanabe et al. reported that the nano-particle anatase phase

* Corresponding author at: Clean Fuels and Catalysis Program, the EMS Energy Institute, and Department of Energy and Mineral Engineering, 209 Academic Projects Building, The Pennsylvania State University, University Park, PA 16802, USA.
Tel.: +1 814 863 4466; fax: +1 814 865 3248.
E-mail address: csong@psu.edu (C.S. Song).

0920-5861/$ – see front matter © 2009 Elsevier B.V. All rights reserved.
doi:10.1016/j.cattod.2009.05.002

was dominant in this TiO_2-based adsorbent [17]. The sulfur removing capacity of this adsorbent was improved by the oxidative pretreatment with air, but decreased by the reductive pretreatment with H_2 [17].

However, the adsorption site and structural dependence of thiophenic compound adsorption over the TiO_2-based materials remains to be clarified. Fundamental understanding of the adsorption mechanism of thiophenic compounds over these materials is necessary for better design and development of the high-performance adsorbents, as well as development of the high-performance catalysts for oxidative desulfurization (ODS). Previous computational works studied thiophenic compounds adsorption over MoS_2-based materials as catalysts [18–21] and TiO_2 rutile as support [22] in HDS. These prior studies provide some guidance in considering the potential adsorption sites and adsorption conformations.

In the present study, first principle calculations by density functional theory (DFT) method were conducted to clarify the adsorption mechanism of thiophenic compounds on the TiO_2-based adsorbents. We first studied the anatase (0 0 1) surface because this surface of anatase is relatively thermodynamically stable, but also reactive in many cases, and therefore has proved useful in other computational study of anatase TiO_2 [23,24]. Other anatase surfaces and mixed titania–ceria surfaces will be studied in our future work, and this initial study is intended to provide benchmark data for these studies. Although thiophenic compounds with steric hindrance are more difficult to be removed and of greater interest in ADS, the thiophene molecule was studied as a model compound as it is the simplest model that captures the S-surface interaction expected to account for adsorption selectivity. The adsorption of thiophene on the perfect, O-poor and O-rich (0 0 1) surfaces of anatase TiO_2 was examined by DFT calculations to gain an insight into the adsorption mechanism of thiophenic compounds on the adsorbents. Such study also benefits the mechanistic study in oxidative desulfurization of liquid hydrocarbon fuels on TiO_2-based catalysts [25–28].

2. Computational methods

Calculations were carried out using the Vienna *ab initio* Simulation Program (VASP), an *ab initio* total-energy and molecular dynamics program developed at the Institute for Material Physics at the University of Vienna [29–31]. The strongly oscillating wave functions of core electrons were represented using the projector augmented wave (PAW) method [32]. Plane wave basis sets with a cut-off energy of 475 eV were used to expand the wave functions of valence electrons with valence configurations for titanium being $3p^6 4s^2 3d^2$, for oxygen $2s^2 2p^4$, for carbon $2s^2 2p^2$, for sulfur $3s^2 3p^4$ and for H $1s^1$. The Perdew–Wang 91 (PW91) form was used for the generalized gradient approximation (GGA) for exchange and correlation potential [33]. A $13 \times 13 \times 13$ Monkhorst–Pack [34] *k*-point mesh was used for the bulk anatase unit cell optimization and a $3 \times 3 \times 1$ *k*-point mesh was used for the (2×2) supercell surface. The electronic self-consistent field was converged to 1×10^{-4} eV and the structural optimization was continued until the forces on all atoms were less than 0.05 eV/Å. Bader charge analysis was used for all the partial charge calculations [35]. The dipole moment along the surface normal direction was calculated within the electronic cycle and corrections were made for these spurious slab-to-slab interactions. Corrections were found to be small in all cases. All calculations were performed spin-polarized.

Adsorption of thiophene on the anatase (0 0 1) surfaces was investigated starting from configurations suggested in the previous literature regarding the coordination geometries of thiophene with metal species in organometallic complexes [8]. The most stable adsorption configurations should be those with the most exothermic adsorption energy. The adsorption energies (E_{ad}) were computed by subtracting the energies of the optimized thiophene molecule ($E_{thiophene}$) and adsorbent bare slab (E_{slab}) from the optimized thiophene-slab complex ($E_{thiophene\text{-}slab}$), as shown below:

$$E_{ad} = E_{thiophene\text{-}slab} - (E_{thiophene} + E_{slab}) \quad (1)$$

A negative E_{ad} value indicates an exothermic adsorption process. There might be an absolute deviation between the absolute E_{ad} values estimated by the calculations and experimental values [36,37]. However, our main interest in this work is to identify the qualitative trends on the basis of the relative adsorption energetic of different adsorption sites, and such an absolute deviation may not affect the results from the comparison of their relative values.

3. Results and discussion

3.1. Anatase unit cell and (0 0 1) surface

The unit cell of anatase was built first by using the experimental lattice parameters from the literature. After the optimization of the bulk volume and the atom positions, the crystal parameters ($a = b = 3.778$ Å, $c = 9.868$ Å) of the unit cell were obtained, which are close to the experimental values ($a = b = 3.782$ Å, $c = 9.502$ Å) reported in the literature [38] and in agreement with the previous theoretical calculation [39], indicating that the computed unit cell for the anatase (0 0 1) surface simulation is reasonable.

The anatase (0 0 1) surface, as shown in Fig. 1, is composed of oxygen and titanium atoms in different O–Ti–O atomic layers. A set of three O–Ti–O atomic layers makes up one stoichiometric layer. There are twofold coordinated oxygen (O-2) atoms and fivefold coordinated titanium (Ti-5) atoms in the top layer. The whole super cell of (2×2) consists of the four stoichiometric layers, with the first two layers relaxed and the bottom two frozen at the optimized bulk anatase positions. A vacuum layer of 15 Å (in the [0 0 1]-direction perpendicular to the surface) above the surface was included, for the adsorption space and to minimize slab-to-slab interactions. The displacements of some surface atoms in the relaxed layers were calculated. Along the [0 0 1] direction, Ti-5 and

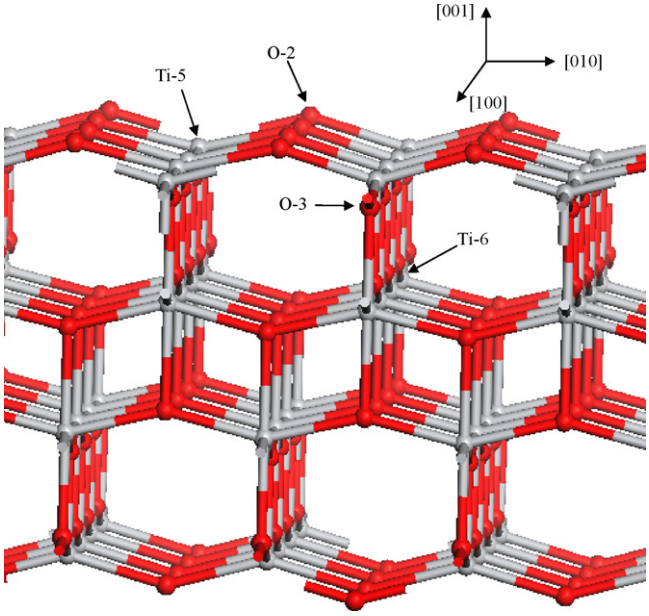

Fig. 1. Anatase (0 0 1) surface, red ball: oxygen, grey ball: titanium. (For interpretation of the references to color in this figure legend, the reader is referred to the web version of the article.)

O-3 atoms have a negative displacement, while O-2 atom has a positive displacement. Along the [1 0 0] direction, the mirror plane symmetry is broken because the two bond lengths between Ti-5 and O-3 become inequivalent. These results are consistent with the results reported in the literature [23,39] using PBE or B3LYP as functionals. Bader charge analysis showed less positive charges (+2.21) on the Ti-5 than the Ti-6 inside the slab (+2.32), and less negative charges (−1.08) on the O-2 than the O inside the slab (−1.16). These results are expected because the atoms on the surface are less saturated and more reactive than the atoms inside the slab.

3.2. Adsorption of thiophene on perfect anatase (0 0 1) surface

Several adsorption geometries of thiophene on perfect anatase (0 0 1) surface, including η^1S, S-μ3, η^2, η^4, and η^5 [8,40,41], were examined and calculated. Among all these configurations, the η^1S bonded with Ti-5 on the surface, as shown in Fig. 2, gave the strongest adsorption energy of −5.4 kcal/mol. This adsorption is dominantly through the interaction between the S atom in thiophene and the Ti-5 cation on the surface. Although this η^1S coordination locates at the global potential energy minimum site on the potential surface of the adsorption, the calculated adsorption energy is low.

3.3. Adsorption of thiophene on O-poor anatase (0 0 1) surface

In many cases, vacancies on the adsorbent surface may be the adsorbent sites [21,22,42]. In order to clarify whether O-vacancies on the anatase (0 0 1) surface play an important role in the adsorption process, the O-poor anatase (0 0 1) (with the O-vacancies) surface was built by removing 25% of the atoms in the bridging O-2 rows of the first layer. The formation energy of an oxygen vacancy was estimated as follows:

$$E_f(\text{O-Vac}) = E(\text{O-poor slab}) + \frac{1}{2}E(O_2) - E(\text{perfect slab}) \quad (2)$$

where $E(O_2)$ is the energy of gas phase O_2 molecule at 0 K. Spin-polarized calculations were conducted and the difference in the numbers of spin up electrons and spin down electrons was found to be 0.22 for the O-poor surface. The formation of the vacancy is highly endothermic, with E_f(O-Vac) value of +94.4 kcal/mol.

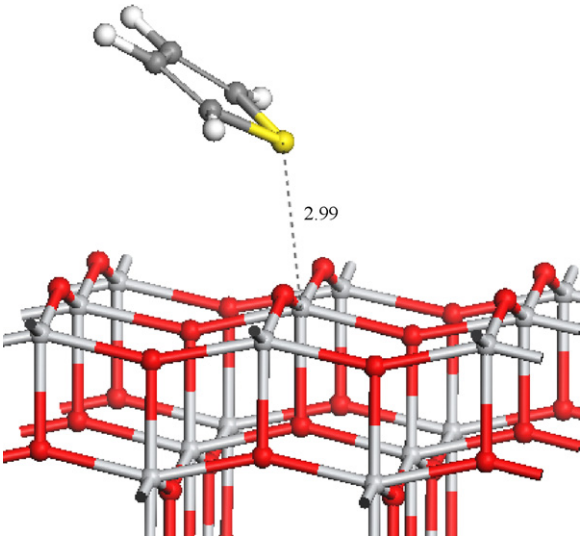

Fig. 2. The adsorption conformation of thiophene on perfect anatase (0 0 1) surface. In thiophene: dark grey spheres-C, yellow sphere-S, white spheres-H. The number indicates the distance (Å) between atoms. (For interpretation of the references to color in this figure legend, the reader is referred to the web version of the article.)

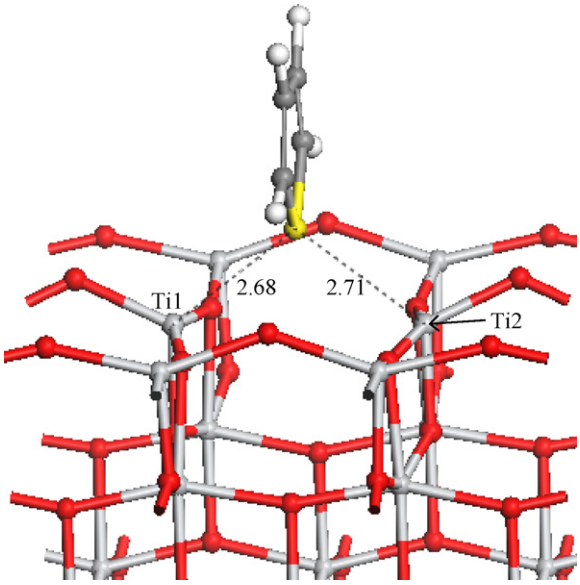

Fig. 3. The adsorption conformation of thiophene on the O-poor anatase (0 0 1) surface.

Several potential adsorption configurations were examined. Fig. 3 shows the most stable adsorption configuration of thiophene on the O-poor surface, in which thiophene interacts with the surface by two S-Ti bonds, where the S atom occupies the O vacancy. A similar configuration was reported by Liu et al. in their study of thiophene adsorption over the rutile surface [22].

The estimated adsorption energy for thiophene on the O vacancy is −7.8 kcal/mol. The difference in the numbers of spin up electrons and spin down electrons is 1.11 after the adsorption, with the polarized spins locating on the two less saturated Ti atoms. Due to the broken mirror plane symmetry observed on relaxed (0 0 1) surface, the distances between S atom in thiophene and the two neighboring unsaturated Ti-5 on the surface are inequivalent, being 2.68 Å and 2.71 Å, respectively. These distances are longer than the typical Ti–S bonding length reported in studies of titanocene sulfido complex: 2.2 Å [43]. The S–C bond in the thiophene molecule increases from initial 1.72 Å to 1.73 Å after the adsorption. Bader charge analysis on each atom indicated little electron transfer between the thiophene molecule and the surface.

3.4. Adsorption of thiophene on O-rich anatase (0 0 1) surface

An over-oxidized surface may arise from the activation of the O_2 to form an O-rich anatase (0 0 1) surface. In order to examine the role of extra oxygen atoms on the surface in the adsorption, two models of O-rich anatase (0 0 1) surface were built, one with a dissociated oxygen molecule, and the other with an associated oxygen molecule. The two O-rich (1 0 0) surfaces after the energy minimization are shown in Fig. 4a and b, respectively. For convenience in the later discussion, these two types of the O-rich surface are denoted as O-rich (*dis*) and O-rich (*mol*), respectively. The configuration of O-rich (*dis*) is similar to the bridging superoxo coordination mode of dinuclear oxygen radicals on TiO_2 [25], whereas the configuration of O-rich (*mol*) is similar to the peroxo coordination mode of dinuclear oxygen radicals on TiO_2 [25]. Both coordination modes were proposed previously by Antcliff et al. on the basis of X-band EPR spectroscopy analysis. The formation energies of these two modes were calculated using spin-polarized methods as shown below:

$$E_f(\text{superoxo}) = E(\text{O-rich}\,(dis)) - E(\text{perfect slab}) - E(O_2), \quad (3)$$

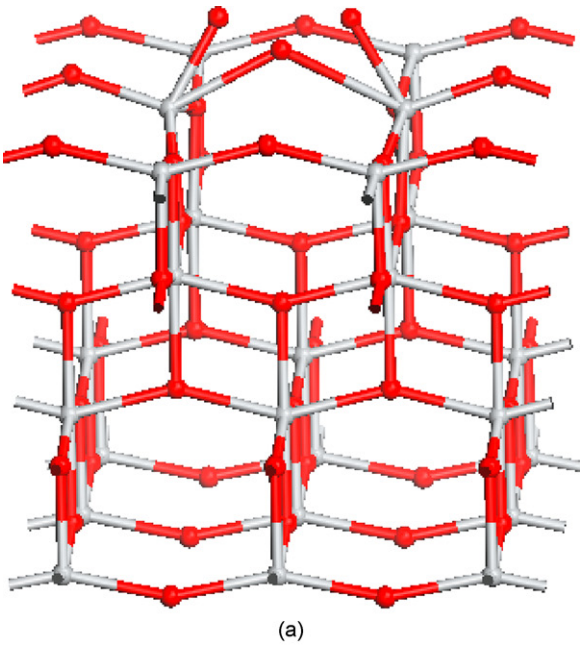

Fig. 4. The O-rich anatase (0 0 1) surfaces (a) with a dissociated oxygen molecule (O-rich (*dis*)), and (b) with an associated oxygen molecule (O-rich (*mol*)).

and

$$E_f(\text{peroxo}) = E(\text{O-rich}\,(mol)) - E(\text{perfect slab}) - E(O_2). \quad (4)$$

The calculated spin state of O-rich (*dis*) is singlet; while the calculated spin state of O-rich (*mol*) is triplet. The formation of O-rich (*dis*) was an endothermic process with E_f = 5.9 kcal/mol, while the formation of O-rich (*mol*) was an exothermic process with E_f = −11.8 kcal/mol. Compared to the energy requirement for formation of the O vacancy, the generation of the O-rich surfaces is more favorable on a 0 K internal energy basis, while of the two types of O-rich planes, the generation of O-rich (*mol*) is thermodynamically preferred. The 0 K internal energy change upon adsorption was modified to a Gibbs free energy change by making zero-point vibrational energy and gas phase O_2 entropy corrections, as described by Mayernick and Janik [44]. At ambient temperature, the estimated Gibbs free energies (ΔG) for O-rich (*dis*) and O-rich (*mol*) were +14.8 kcal/mol and −5.0 kcal/mol, respectively. It must be noted that all the formation energies of O-poor and O-rich surfaces reported in this study are not direct analogs to experimental enthalpies, due to the overestimation of the O_2 binding energy given by DFT [45]. However, the overestimation will not affect relative values of E_f.

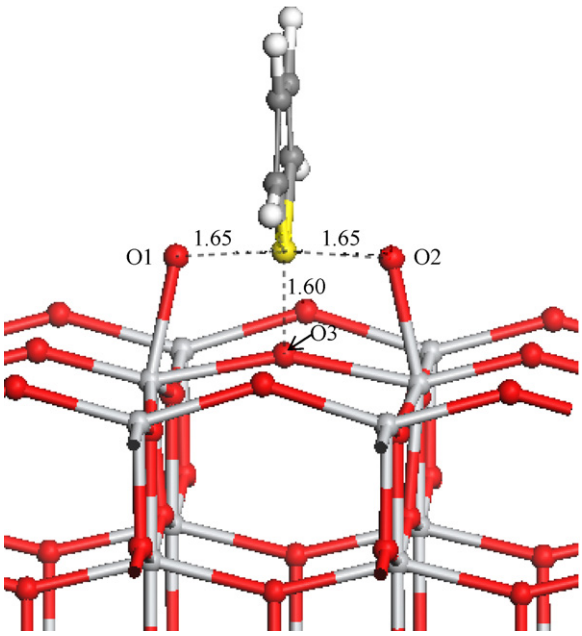

Fig. 5. The adsorption conformation of thiophene on O-rich (*dis*) anatase (0 0 1) surface, on which the extra oxygen atoms are dissociatively adsorbed on the (0 0 1) surface.

The conformations of thiophene interacting with these two surfaces are shown in Figs. 5 and 6, respectively. Different from the adsorption over the perfect surface and the O-poor surface, the saturated Ti sites do not contribute to the adsorption any more. Instead, thiophene strongly interacts with the extra O atoms through S–O bonds over the O-rich surface. The adsorption energies were calculated as Eq. (1), where the slab could be O-rich (*dis*) or O-rich (*mol*) in this case.

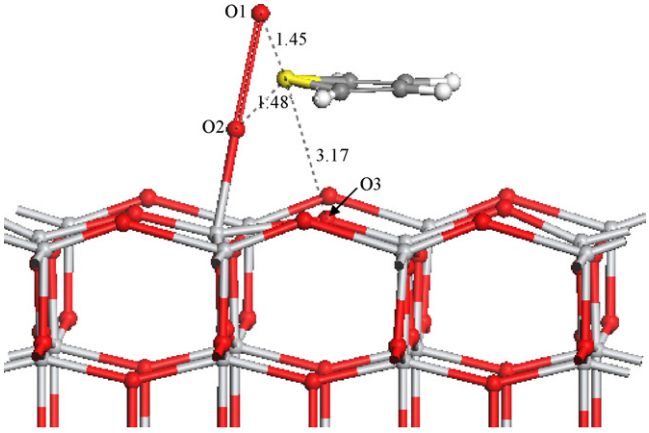

Fig. 6. The adsorption conformation of thiophene on O-rich (*mol*) anatase (0 0 1) surface, on which the extra oxygen atoms are molecularly adsorbed on the perfect surface.

Table 1
Comparison in the adsorption energies, adsorption conformations, and Bader charge for adsorption of thiophene on the perfect, O-poor, and O-rich surfaces.

Anatase (0 0 1)	Perfect	O-poor	O-rich (*dis*)	O-rich (*mol*)
Adsorption energy (kcal/mol)	−5.4	−7.8	−44.6	−51.4
Adsorption bonding length (Å)	S-Ti 2.99	S-Ti1 2.68, S-Ti2 2.71	S-O1 1.65, S-O3 1.60	S-O1 1.45, S-O2 1.48, S-O3 3.17
C–S bond length (Å), 1.72 in free thiophene	1.72	1.73	1.79	1.78
Bader partial charge on thiophene	+0.04	−0.10	+3.87	+3.83

For adsorption on the O-rich (*dis*), the sulfur in thiophene is bonded with the three neighboring oxygen atoms (two are the extra ones and the other is a bridging oxygen on the surface), with the calculated adsorption energy of −44.6 kcal/mol and singlet spin state. As shown in Fig. 5, O1 and O2 are identical and their distances to the S in thiophene are the same, being 1.65 Å. The S–O3 bond length is 1.60 Å. Due to the formation of these three S–O bonds, the C–S bond strength becomes weaker, with the increase of bond length from 1.72 Å to 1.79 Å. The Bader charge analysis indicates that about 3.87 electrons were transferred from the thiophene molecule to the oxygen atoms on the surface, confirming a formal charge change to S^{4+}. The partial charges on O-1 and O-3 are −1.61 and −1.78, respectively.

Interaction between the S atom and the extra O atoms can also be observed in the O-rich (*mol*) conformation, as shown in Fig. 6. O1 and O2, which are the two oxygen atoms of the oxygen molecule adsorbed on the surface, form chemical bonds with the S atom, with the calculated bond length of 1.45 Å and 1.48 Å, respectively. Interaction between the S atom and O3 atom is negligible, with a distance of greater than 3.0 Å. The spin state after the adsorption becomes singlet. Fig. 6 indicates that the adsorption of thiophene on this O-rich (*mol*) forms a sulfone-like surface species. The estimated adsorption energy is −51.4 kcal/mol and the amount of the transferred Bader charges from thiophene to the slab is 3.83 electrons.

3.5. Comparison of the adsorption on different type of anatase (0 0 1) surfaces

Table 1 summarizes the estimated adsorption energies and related bond lengths, as well as the amount of charge transfer due to the adsorption over the anatase surfaces. The adsorption interaction on the surfaces strengthens in the order of: perfect surface < O-poor surface < O-rich (*dis*) surface < O-rich (*mol*) surface. The adsorption results in weakening the S–C bonds in thiophene, especially on the O-rich surfaces. Almost four electrons were transferred from thiophene molecule to the active oxygen atoms on O-rich surfaces.

In both cases of the perfect and the O-poor anatase (0 0 1) surfaces, the adsorption of thiophene is dominantly through the interaction between the Ti cations on the surface and negatively charged S in the thiophene compound. However, the adsorption energy in the latter case is stronger compared to that of the former. What makes the difference is that on the O-poor surface the S atom interacts with two less saturated Ti atoms, due to the occupancy of the S at the O vacancy. Both the O-rich (*dis*) and O-rich (*mol*) surfaces have much stronger adsorption energies. Adsorption on the O-rich surface occurs through S–O interactions and therefore is suggestive of a path to oxidative regeneration, as opposed to the stoichiometric (perfect) or reduced (O-poor) surfaces in which the sulfur in thiophene interacts with Ti atoms in the adsorbed state. This finding helps to explain our previous experimental observation [16] that TiO_2-based material has good adsorption selectivity for the S-containing compounds in the presence of other fuel components.

The present computational results indicate that the anatase (0 0 1) may be able to activate the oxygen molecule to form an O-rich anatase (0 0 1) plane, which leads to higher adsorption affinity for thiophenic molecules. This finding explains our experimental observation that pretreatment with air improved the adsorption performance of the TiO_2-based adsorbent [17]. Other positive effects of the air-pretreatment, such as cleaning off surface poisons, could also be possible, and were not considered herein. However, pretreatment with nitrogen does not increase the adsorption capacity whereas air-pretreatment does [17], suggesting that the surface oxidation to form the O-rich surface should play a more important role in the improvement of the adsorption performance of TiO_2. The simulation further reveals that thiophene is adsorbed on O-rich anatase (0 0 1) plane to form a sulfone-like surface species. This finding may also provide an insight into the mechanism of the oxidative desulfurization of thiophenic compounds on the TiO_2-based catalysts. The simulation on O-poor surface shows that the O-vacancy formed on anatase (0 0 1) is also able to adsorb a thiophene molecule. Were this site responsible for increased adsorption capacity, the adsorbent pretreated by H_2 must have better adsorption performance than one without the pretreatment. However, our previous experimental study showed that the H_2-pretreatment at 375 °C and ambient pressure did not improve, but rather decreased the adsorption capacity of the adsorbent [17]. The disagreement between the present computational results and previous experimental results might be due to (1) the high energy requirement for formation of the O-vacancy on the anatase (0 0 1) surface [46], and/or (2) the formation of hydroxyl groups and Ti–H bonds on the anatase (0 0 1) surface [47], which saturates the active sites on the surface. More computational studies are necessary to further clarify the importance of surface hydroxylation on thiophene adsorption.

4. Conclusions

On the basis of the present DFT study on the interaction of thiophene with the perfect, O-poor and O-rich anatase (0 0 1) surfaces, the following conclusions may be drawn:

(1) All the adsorption conformations suggested by the present computational chemistry study indicate that adsorption of thiophene on the anatase (0 0 1) surfaces is likely through the S atom in thiophene, which could be one of the reasons for the good selectivity of the TiO_2-based adsorbents observed in our previous experiments.
(2) Thiophene can be adsorbed strongly on the O-rich anatase (0 0 1) surfaces, which are formed by the activation of molecular O_2 on the anatase (0 0 1) surface, via S–O bonds to form a sulfone-like species.
(3) The interaction between thiophene and the perfect or O-poor anatase (0 0 1) surface is relatively weaker than those on the O-rich anatase (0 0 1) surface. The oxygen vacancies on the anatase (0 0 1) surface are unlikely to be the adsorption sites for thiophenic compounds.

Acknowledgements

This work is supported in part by the US National Science Foundation (NSF) and the US Environmental Protection Agency (EPA) joint TSE program, by the U.S. Office of Naval Research (ONR),

and by a fellowship from ConocoPhillips Corp. We gratefully acknowledge the support of ONR Navsea Program Manager Donald Hoffman. We also thank Dr. James Kubicki and Dr. Jonathan P. Mathews of PSU for many helpful discussions and providing a part of computational resource for this study.

References

[1] C.S. Song, X.L. Ma, Appl. Catal. B: Environ. 41 (2003) 207.
[2] J. Larminie, A. Dicks, Fuel Cell Systems Explained, John Wiley, New York, 2000.
[3] B.C. Gates, H. Topsoe, Polyhedron 16 (1997) 3213.
[4] C.S. Song, Catal. Today 86 (2003) 211.
[5] C.S. Song, Catal. Today 77 (2002) 17.
[6] I.V. Babich, J.A. Moulijn, Fuel 82 (2003) 607.
[7] D.H. Wang, E.W.H. Qian, H. Amano, K. Okata, A. Ishihara, T. Kabe, Appl. Catal. A: Gen. 253 (2003) 91.
[8] X.L. Ma, L. Sun, C.S. Song, Catal. Today 77 (2002) 107.
[9] S. Velu, X.L. Ma, C.S. Song, Ind. Eng. Chem. Res. 42 (2003) 5293.
[10] S. Velu, X.L. Ma, C.S. Song, M. Namazian, S. Sethuraman, G. Venkataraman, Energy Fuels 19 (2005) 1116.
[11] A.J. Hernndez-Maldonado, R.T. Yang, J. Am. Chem. Soc. 126 (2004) 992.
[12] A.J. Hernndez-Maldonado, F.H. Yang, G. Qi, R.T. Yang, Appl. Catal. B: Environ. 56 (2005) 111.
[13] X.L. Ma, M. Sprague, C.S. Song, Ind. Eng. Chem. Res. 44 (2005) 5768.
[14] S. Watanabe, S. Velu, X.L. Ma, C.S. Song, Am. Chem. Soc. Div. Fuel Chem. Prepr. 48 (2003) 695.
[15] A.N. Zhou, X.L. Ma, C.S. Song, J. Phys. Chem. B 110 (2006) 4699.
[16] S. Watanabe, X.L. Ma, C.S. Song, Am. Chem. Soc. Div. Fuel Chem. Prepr. 49 (2004) 511.
[17] (a) S. Watanabe, X.L. Ma, C.S. Song, Characterization of structural and surface properties of nanocrystalline TiO_2–CeO_2 mixed oxides by XRD, XPS, TPR and TPD. J. Phys. Chem. C. (2009), in press.;
(b) S. Watanabe, Adsorption of thiophenic compounds on TiO_2–CeO_2 mixed oxide: study of adsorbent and adsorption mechanism, PhD Thesis, The Pennsylvania State University, 2007.
[18] D.C. Sorescu, D.S. Sholl, A.V. Cugini, J. Phys. Chem. B 107 (2003) 1988.
[19] H. Yang, C. Fairbridge, Z. Ring, Enery Fuels 17 (2003) 387.
[20] S. Cristol, J.-F. Paul, E. Payen, D. Bougeard, F. Hutschka, S. Clemendot, J. Catal. 224 (2004) 138.
[21] S. Cristol, J.-F. Paul, C. Schovsbo, E. Veilly, E. Payen, J. Catal. 239 (2006) 145.
[22] G. Liu, J.A. Rodriguez, J. Hrbek, B.T. Long, D.A. Chen, J. Mol. Catal. A: Chem. 202 (2003) 215.
[23] A. Beltran, J.R. Sambrano, M. Calatayud, F.R. Sensato, J. Andres, Surf. Sci. 490 (2001) 116.
[24] A. Ignatchenko, D.G. Nealon, R. Dushane, K. Humphries, J. Mol. Catal. A: Chem. 256 (2006) 57.
[25] K.L. Antcliff, D.M. Murphy, E. Griffiths, E. Giamello, Phys. Chem. Chem. Phys. 5 (2003) 4306.
[26] L. Cedeno-Caero, H. Gomez-Bernal, A. Fraustro-Cuevas, H.D. Guerra-Gomez, R. Cuevas-Garcia, Catal. Today 133 (2008) 244.
[27] S.H. Cui, F. Ma, Y.Q. Wang, React. Kinet. Catal. Lett. 92 (2007) 155.
[28] S. Matsuzawa, J. Tanaka, S. Sato, T. Ibusuki, J. Photochem. Photobiol. A 149 (2002) 183.
[29] G. Kresse, J. Furthmuller, Comput. Mater. Sci. 6 (1996) 15.
[30] G. Kresse, J. Furthmuller, Phys. Rev. B 54 (1996) 11169.
[31] G. Kresse, J. Hafner, Phys. Rev. B 47 (1993) 558.
[32] G. Kresse, D. Joubert, Phys. Rev. B 59 (1999) 1758LP.
[33] J.P. Perdew, J.A. Chevary, S.H. Vosko, K.A. Jackson, M.R. Pederson, D.J. Singh, C. Fiolhais, Phys. Rev. B 46 (1992) 6671.
[34] H.J. Monkhorst, J.D. Pack, Phys. Rev. B 13 (1976) 5188LP.
[35] (a) G. Henkelman, A. Arnaldsson, H. Jonsson, Comput. Mater. Sci. 36 (2006) 254; (b) E. Sanville, S.D. Kenny, R. Smith, G. Henkelman, J. Comput. Chem. 28 (2007) 899.
[36] R.A. van Santen, M. Neurock, Catal. Rev. Sci. Eng. 37 (1995) 557.
[37] N. Lopez, F. Illas, N. Rosh, G. Pacchioni, J. Chem. Phys. 110 (1999) 4873.
[38] U. Diebold, Surf. Sci. Rep. 48 (2003) 53.
[39] M. Lazzeri, A. Vittadini, A. Selloni, Phys. Rev. B 63 (2001) 155409.
[40] R.A. Sanchez-Delgado, J. Mol. Catal. 86 (1994) 287.
[41] R.J. Angelici, Bull. Soc. Chim. Beld. 104 (1995) 268.
[42] X.L. Ma, H.H. Schobert, J. Mol. Catal. A: Chem. 160 (2000) 409.
[43] Z.K. Sweeney, J.L. Polse, R.A. Andersen, R.G. Bergman, M.G. Kubinec, J. Am. Chem. Soc. 119 (1997) 4543.
[44] A.D. Mayernick, M.J. Janik, J. Phys. Chem. C 221 (2008) 14955.
[45] L. Wang, T. Maxisch, G. Ceder, Phys. Rev. B 73 (2006) 195107.
[46] A. Bouzoubaa, A. Markovits, M. Calatayud, C. Minot, Surf. Sci. 583 (2005) 107.
[47] C. Arrouvel, H. Toulhoat, M. Breysse, P. Raybaud, J. Catal. 226 (2004) 260.